



3 4456 0330569 8

ORNL/TM-11545



OAK RIDGE
NATIONAL
LABORATORY

MARTIN MARIETTA

ATF Edge Plasma Turbulence Studies Using a Fast Reciprocating Langmuir Probe

T. Uckan
C. Hidalgo
J. D. Bell
J. H. Harris
J. L. Dunlap
G. R. Dyer
P. K. Mioduszewski
J. B. Wilgen
Ch. P. Ritz
A. J. Wootton
T. L. Rhodes
K. Carter

OAK RIDGE NATIONAL LABORATORY
CENTRAL RESEARCH LIBRARY
CIRCULATOR SECTION
JASPER ROOM 173
LIBRARY LOAN COPY
DO NOT TRANSFER TO ANOTHER PERSON
If you wish someone else to see this
report, send its name with report and
the library will arrange a loan.

MANAGED BY
MARTIN MARIETTA ENERGY SYSTEMS, INC.
FOR THE UNITED STATES
DEPARTMENT OF ENERGY

This report has been reproduced directly from the best available copy.

Available to DOE and DOE contractors from the Office of Scientific and Technical Information, P.O. Box 62, Oak Ridge, TN 37831; prices available from (615) 576-8401, FTS 626-8401

Available to the public from the National Technical Information Service, U.S. Department of Commerce, 5285 Port Royal Rd., Springfield, VA 22161.

This report was prepared as an account of work sponsored by an agency of the United States Government. Neither the United States Government nor any agency thereof, nor any of their employees, makes any warranty, express or implied, or assumes any legal liability or responsibility for the accuracy, completeness, or usefulness of any information, apparatus, product, or process disclosed, or represents that its use would not infringe privately owned rights. Reference herein to any specific commercial product, process, or service by trade name, trademark, manufacturer, or otherwise, does not necessarily constitute or imply its endorsement, recommendation, or favoring by the United States Government or any agency thereof. The views and opinions of authors expressed herein do not necessarily state or reflect those of the United States Government or any agency thereof.

Fusion Energy Division

**ATF EDGE PLASMA TURBULENCE STUDIES USING A FAST
RECIPROCATING LANGMUIR PROBE**

T. Uckan
C. Hidalgo*
J. D. Bell
J. H. Harris
J. L. Dunlap
G. R. Dyer
P. K. Mioduszewski
J. B. Wilgen

Ch. P. Ritz
A. J. Wootton
T. L. Rhodes
K. Carter
Fusion Research Center, The University of Texas, Austin

*Permanent address: Asociación EURATOM/CIEMAT, Madrid, Spain.

Date published: January 1991

Prepared for the
Office of Fusion Energy
under Budget Activity No. AT 10 10 15 B

Prepared by
OAK RIDGE NATIONAL LABORATORY
Oak Ridge, Tennessee 37831-6285
managed by
MARTIN MARIETTA ENERGY SYSTEMS, INC.
for the
U.S. DEPARTMENT OF ENERGY
under contract DE-AC05-84OR21400



3 4456 0330569 8

CONTENTS

ABSTRACT	v
1. INTRODUCTION	1
2. EXPERIMENTAL SETUP	1
3. RESULTS AND DISCUSSION	3
4. CONCLUSION	10
ACKNOWLEDGMENTS	12
REFERENCES	13

ABSTRACT

Electrostatic turbulence on the edge of the Advanced Toroidal Facility (ATF) toratron is investigated experimentally with a fast reciprocating Langmuir probe (FRLP) array. Initial measurements of plasma electron density n_e and temperature T_e and fluctuations in density (\tilde{n}_e) and plasma floating potential ($\tilde{\phi}_f$) are made in electron cyclotron heated plasmas at 1 T. At the last closed flux surface (LCFS, $r/\bar{a} \sim 1$), $T_e \approx 20\text{--}40$ eV and $n_e \approx 10^{12}$ cm $^{-3}$ for a line-averaged electron density $\bar{n}_e = (3\text{--}6) \times 10^{12}$ cm $^{-3}$. Relative fluctuation levels, as the FRLP is moved into core plasma where $T_e > 20$ eV, are $\tilde{n}_e/n_e \approx 5\%$ and $e\tilde{\phi}_f/T_e \approx 2\tilde{n}_e/n_e$ about 2 cm inside the LCFS. The observed fluctuation spectra are broadband (40–300 kHz) with $\bar{k}\rho_s \leq 0.1$, where \bar{k} is the wavenumber of the fluctuations and ρ_s is the ion Larmor radius at the sound speed. The propagation direction of the fluctuations reverses to the electron diamagnetic direction around $r/\bar{a} < 1$. The phase velocity and the electron drift velocity are comparable ($v_{ph} \sim v_{de}$). The fluctuation-induced particle flux is comparable to fluxes estimated from the particle balance using the H_α spectroscopic measurements. Many of the features seen in these experiments resemble the features of ohmically heated plasmas in the Texas Experimental Tokamak (TEXT).

1. INTRODUCTION

Energy and particle confinement in tokamaks and stellarators is anomalous, and results from the two types of devices show similar dependences on plasma parameters [1]. The study of electrostatic fluctuations [2] in different magnetic configurations may help to identify the underlying physics mechanisms responsible for plasma transport. To investigate the effects of the magnetic configuration on the characteristics of edge turbulence, recent measurements of electrostatic fluctuations at the edge of the Texas Experimental Tokamak (TEXT) [3] have been extended to the Advanced Toroidal Facility (ATF) [4] torsatron. Experimental observations on TEXT indicate that electrostatic fluctuations are the dominant mechanism for energy and particle losses in the edge [3,5]. To understand the driving forces on the edge turbulence in terms of the plasma current and the magnetic configuration, initial edge fluctuation measurements have been carried out on the currentless ATF device with a diagnostic setup similar to that used in the TEXT experiments, that is, a fast reciprocating Langmuir probe (FRLP) array [6].

The FRLP has been used to characterize, from an experimental point of view, the electrostatic turbulence on the edge of the ATF torsatron. The experimental setup and the analysis method are described in Sect. 2. Measurements of plasma electron density n_e , electron temperature T_e , and fluctuations in density (\bar{n}_e) and plasma floating potential ($\tilde{\phi}_f$) at the edge of electron cyclotron heated (ECH) plasmas in ATF are presented and their turbulence characteristics are discussed in Sect. 3. Brief conclusions follow in Sect. 4.

2. EXPERIMENTAL SETUP

The stellarator configuration of the ATF torsatron has a poloidal multipolarity $l = 2$, 12 field periods ($M = 12$), a major radius $R_0 = 2.1$ m, and an average plasma radius $\bar{a} = 0.27$ m. The externally produced currentless magnetic configuration has moderate shear; that is, the central rotational transform ($\nu/2\pi = 1/q$) of 0.3 becomes 1.0 at the last closed flux surface (LCFS). Initial fluctuation measurements in ATF were carried out around the LCFS with the FRLP in ECH plasmas at a magnetic field $B = 1$ T. Plasmas were created using a gyrotron source at 53 GHz with heating power $P = 200$ kW. In these ECH plasmas, a representative range for the line-averaged plasma density is $\bar{n}_e = (3-6) \times 10^{12} \text{ cm}^{-3}$, and the plasma stored energy $W_p \approx 1-2$ kJ.

The FRLP is located one field period away from the instrumented rail limiter [7]. The probe is inserted into the edge plasma from the top, moves 5 cm into the plasma in 50 ms, and remains there about for 40 ms to carry out the fluctuation measurements. The FRLP head consists of a square array of four tips, 0.5 mm in diameter, that are 2 mm long and 2 mm apart. Double Langmuir probe operation of two tips, aligned perpendicular to the local magnetic field, makes it possible to measure the edge plasma n_e , T_e , and \bar{n}_e/n_e profiles inside (about 2 cm) and outside the LCFS, as indicated in Fig. 1. The other two tips are used to measure $\tilde{\phi}_f$ and the wavenumber k perpendicular to the local magnetic field. The data have been analysed using spectral analysis techniques [8]. That is, the fluctuation signals are digitized at 1 MHz, and fast Fourier transform (FFT) is

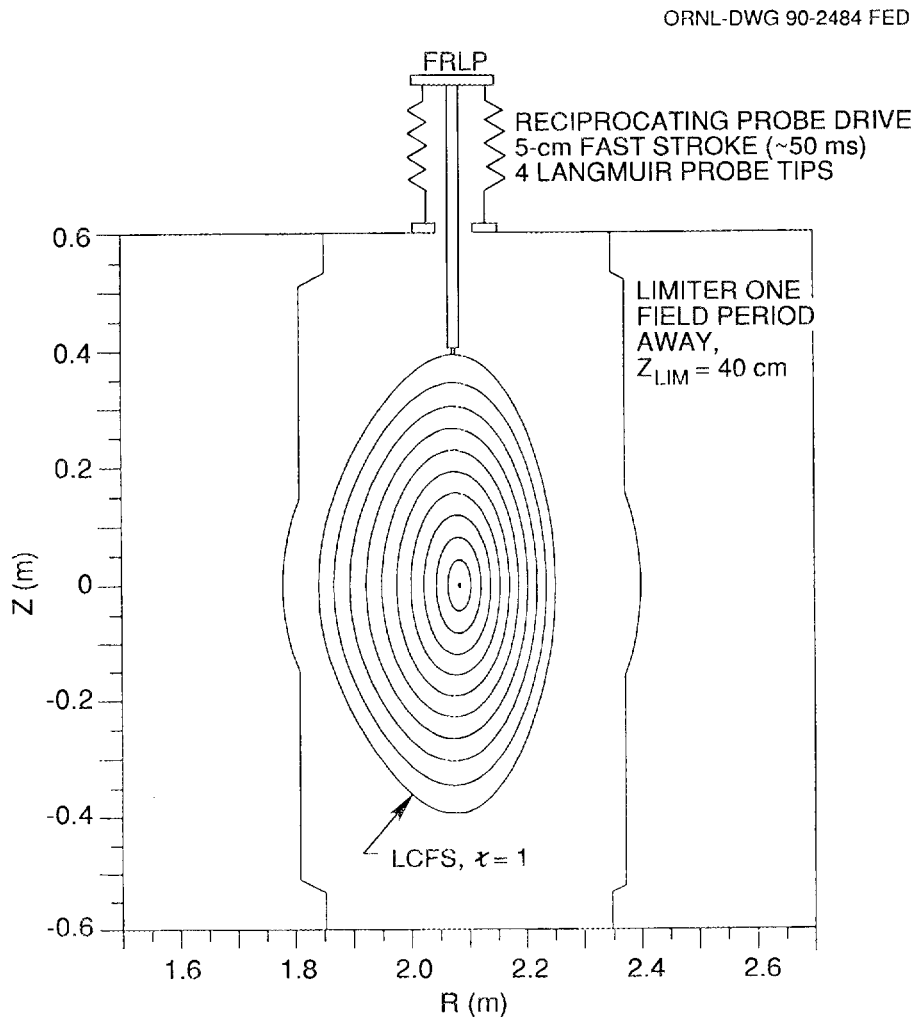


Fig. 1. Constant flux surfaces and the location of the FRLP on ATF.

used to obtain their power spectrum $S(k, \omega)$ as a function of frequency ω and k using the two-probe technique described in ref. [9]. Ensemble averaging of the spectral distribution of the flux $\tilde{\Gamma}(\omega)$, obtained from the correlation of density and plasma potential fluctuations ($\tilde{\phi}_p$), gives the turbulence-induced radial particle flux:

$$\tilde{\Gamma} = \langle \tilde{n}_e \tilde{v}_r \rangle = 2 \sum_{\omega > 0} \tilde{\Gamma}(\omega). \quad (1)$$

Here $\tilde{v}_r = -ik\tilde{\phi}_p/B$ is the radial velocity due to the electrostatic fluctuations, and the frequency-resolved flux is estimated from many independent realizations using a triple correlation technique [10]:

$$\tilde{\Gamma}(\omega) = \text{Re}[\langle -ik(\omega)\tilde{n}_e^*(\omega)\tilde{\phi}_p(\omega) \rangle]/B. \quad (2)$$

Further, to gain an insight into the physical process, $\tilde{\Gamma}(\omega)$ can be expressed as [8]

$$\tilde{\Gamma}(\omega) \approx (k/B)\gamma_{\tilde{n}\tilde{\phi}} n_{\text{rms}} \phi_{\text{rms}} \sin\theta_{\tilde{n}\tilde{\phi}}, \quad (3)$$

where $\gamma_{\tilde{n}\tilde{\phi}}$ is the coherence, $\theta_{\tilde{n}\tilde{\phi}}$ is the phase angle between the density and potential fluctuations, and n_{rms} and ϕ_{rms} are the rms values of the fluctuations.

3. RESULTS AND DISCUSSION

Spatial profiles of the edge plasma density and temperature and the plasma floating potential ϕ_f are shown in Fig. 2 for $0.95 < r/\bar{a} < 1.15$. These measurements were made during the steady-state phase of the plasma discharge. The plasma potential ϕ_p may be estimated from the measurements of ϕ_f and T_e as $\phi_p \approx \phi_f + \delta_p T_e$, where δ_p depends on the probe material, the heat load on the probe, the ion species and its temperature, and the secondary electron emission coefficient. Typically, $\delta_p \sim 1-3$ for hydrogen plasmas [11]. Around the LCFS, $r/\bar{a} \approx 1$, the plasma parameters are $n_e = (1-1.2) \times 10^{12} \text{ cm}^{-3}$ and $T_e = 30-40 \text{ eV}$. The characteristic density and temperature scale lengths are $L_n = [-(1/n_e) \times (dn_e/dr)]^{-1} \approx 3-4 \text{ cm}$ and $L_T \approx 2L_n$, respectively. These values are comparable (within a factor of 2) to those for ohmically heated plasmas in TEXT at 2 T [3].

Typical values for the normalized density (\tilde{n}_e/n_e) and potential ($\tilde{\phi}_f/T_e$) fluctuations (see Fig. 3 for profiles) around the LCFS are $\tilde{n}_e/n_e \approx 0.05-0.1$ and $\tilde{\phi}_f/T_e \approx 0.1-0.2$, which

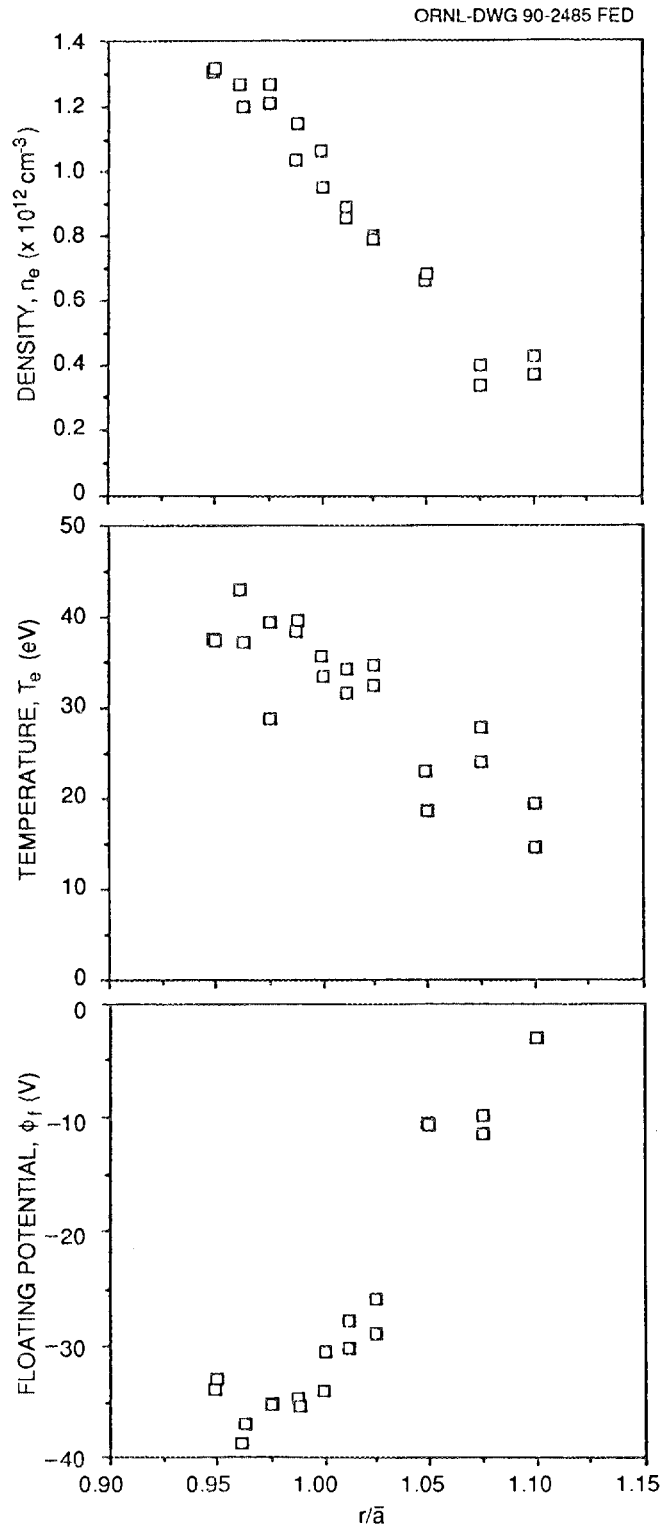


Fig. 2. Spatial profiles of the ATF edge plasma density, temperature, and floating potential.

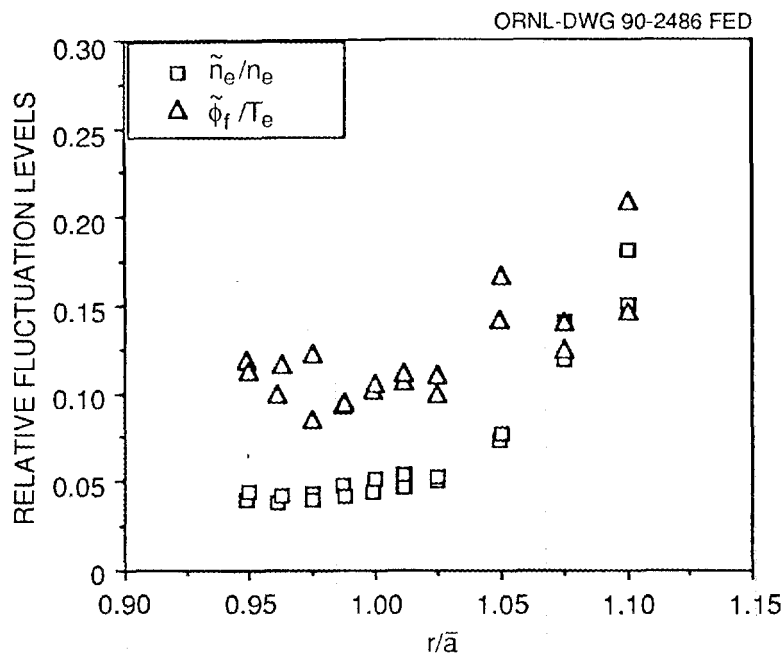


Fig. 3. Relative fluctuation levels for edge density and potential.

are lower than those in TEXT plasmas [3]. Although the correlation between $\tilde{\phi}_f$ and temperature fluctuations \tilde{T}_e in ATF is not yet known, the contribution of \tilde{T}_e to $\tilde{\phi}_p$ has been neglected because the measured values of \tilde{T}_e on TEXT were relatively small ($\tilde{T}_e/T_e \approx 0.4\tilde{n}_e/n_e$) [12]. Fluctuation levels decrease as the probe is moved into the core plasma, where $T_e > 20$ eV and $\tilde{\phi}_f/T_e \approx 2\tilde{n}_e/n_e$ at $r/\bar{a} \approx 0.95$.

Fluctuation spectra of \tilde{n}_e and $\tilde{\phi}_f$ have been examined for frequencies up to 400 kHz. Observed wavenumber-frequency power spectra $S(k, \omega)$ are broadband and mostly in the range 40–300 kHz (as seen in Figs. 4 and 5). The estimated mean value of the wavenumbers from the two probe measurements is $\bar{k} = 1\text{--}3 \text{ cm}^{-1}$, which satisfies $\bar{k}\rho_s \approx 0.05\text{--}0.1$, where ρ_s is the ion Larmor radius at the sound speed, as observed in TEXT [3]. Analysis of the wavenumber spectra shows that inside the LCFS the spectral width σ_k , the rms deviation about \bar{k} , decreases with increasing local electron temperature (Fig. 6), indicating that the correlation length $L_c = 1/\sigma_k$ increases with temperature [13] and typically $L_c \approx 1$ cm, which is much larger than the probe tip separation, for $T_e > 35$ eV. The integrated potential fluctuation power spectra $S(\omega)$ and $S(k)$ decrease for large $\omega/2\pi$ (>200 kHz) and k (as illustrated in Fig. 5) with dependences given by $S(\omega) \sim \omega^{-\alpha}$ and $S(k) \sim k^{-\beta}$, where $\alpha \sim \beta \approx 4 \pm 1$, with a possible deviation from the true shape but a

ORNL-DWG 90-2488 FED

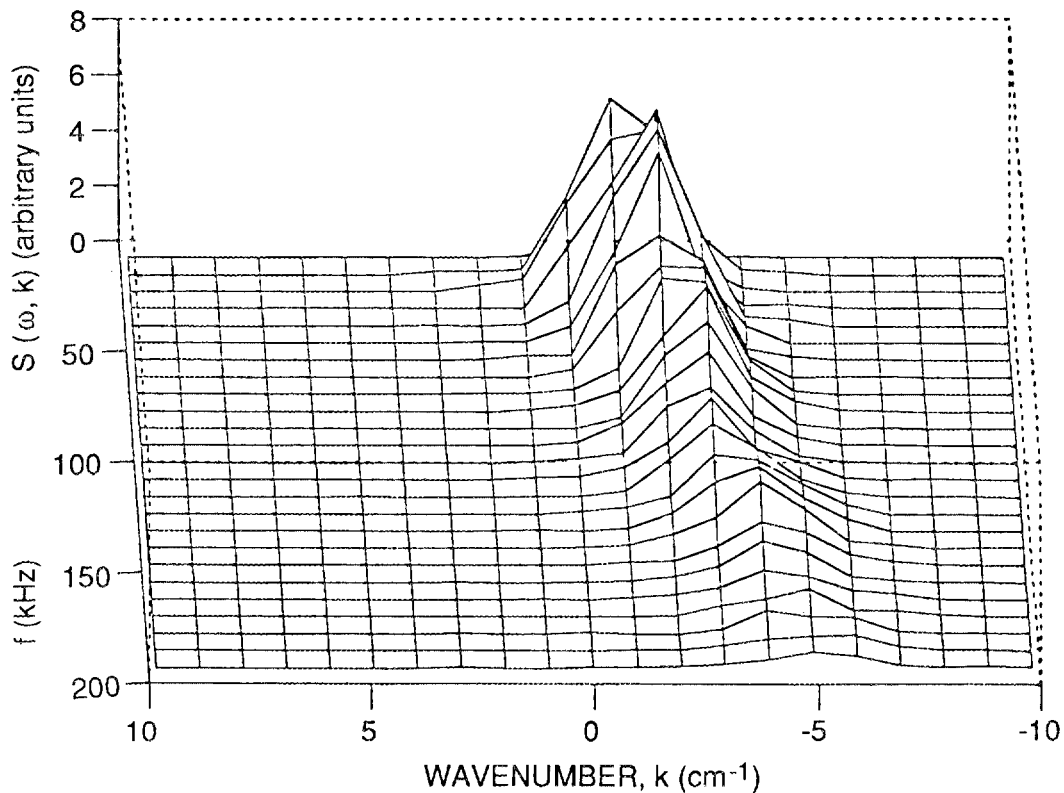


Fig. 4. Wavenumber-frequency power spectrum for potential fluctuations.

ORNL-DWG 90-2531 FED

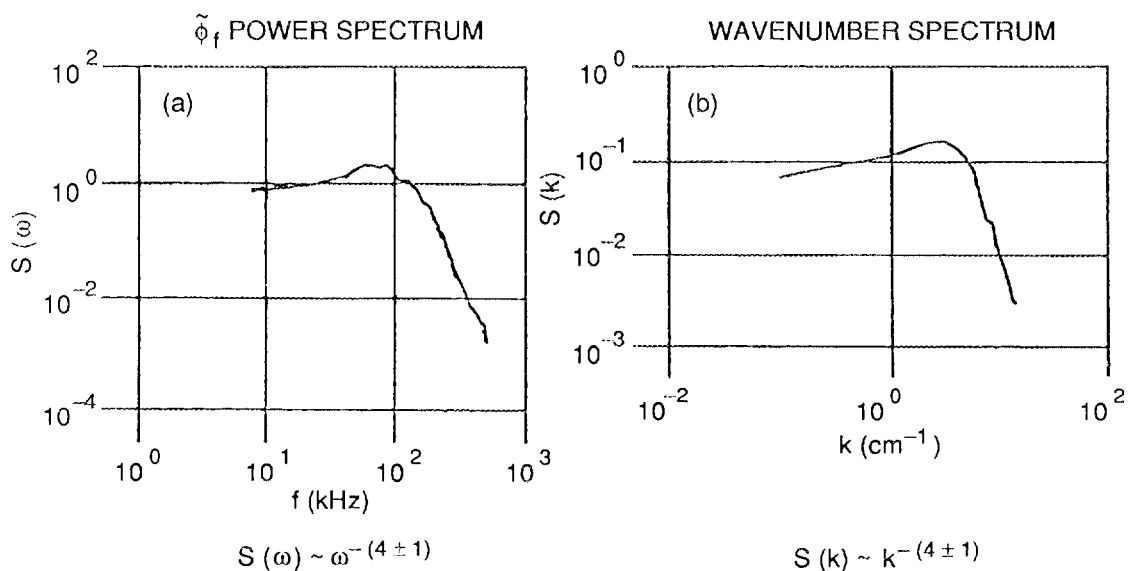


Fig. 5. (a) Power spectrum of the potential fluctuations. (b) Wavenumber spectrum $S(k)$.

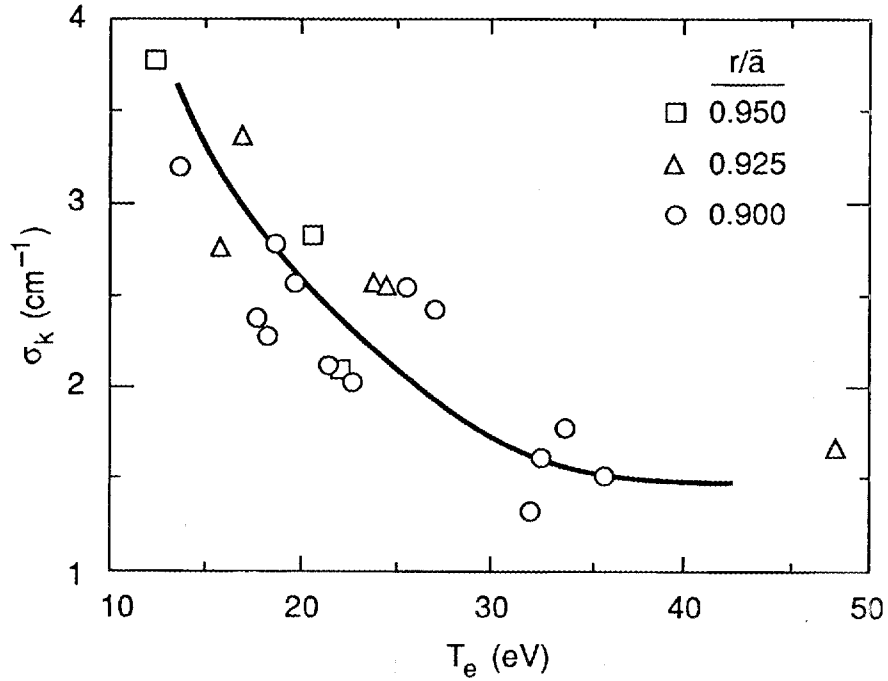


Fig. 6. Variations of σ_k with T_e inside the LCFS.

reliable determination of \bar{k} and σ_k [9,14]. The shape of the \bar{n}_e spectrum is generally similar to that of $\tilde{\Phi}_f$.

The fluctuation-induced particle flux is estimated from Eqs. (1) and (2) by taking $\tilde{\Phi}_p \approx \tilde{\Phi}_f$. The coherence between the density and the floating potential fluctuations is $\gamma_{\bar{n}\tilde{\Phi}} \approx 0.8$ up to 150 kHz, dropping to ~ 0.2 beyond 250 kHz, and the corresponding phase angle is $\theta_{\bar{n}\tilde{\Phi}} \approx 70^\circ$ around 150 kHz. The frequency-resolved particle flux $\tilde{\Gamma}(\omega)$ is dominated by frequencies below 250 kHz (Fig. 7) and reaches a maximum at 100–150 kHz, where the phase angle has its maximum. The spatial profile of the total particle flux $\tilde{\Gamma}$, Eq. (1), is given in Fig. 8 for two representative line-averaged densities $\bar{n}_e = 3.5 \times 10^{12} \text{ cm}^{-3}$ and $5.5 \times 10^{12} \text{ cm}^{-3}$. The radial flux is always outward and at the LCFS has a value $\tilde{\Gamma} \sim 3 \times 10^{15} \text{ cm}^{-2} \cdot \text{s}^{-1}$ for $\bar{n}_e = 3.5 \times 10^{12} \text{ cm}^{-3}$ and $1.2 \times 10^{15} \text{ cm}^{-2} \cdot \text{s}^{-1}$ for $\bar{n}_e = 5.5 \times 10^{12} \text{ cm}^{-3}$. For the nearly flat core density profiles observed in ATF, the corresponding fluctuation-induced particle confinement times, assuming that $\tilde{\Gamma}$ is constant on flux surfaces, are $\tau_p = (\bar{a}/2)\bar{n}_e/\tilde{\Gamma} \sim 16 \text{ ms}$ and 60 ms , respectively. The associated local density diffusion coefficient is $D_n = \tilde{\Gamma}L_n/n_e \sim 1 \times 10^4 \text{ cm}^2 \cdot \text{s}^{-1}$, where $n_e(\text{edge}) \sim 10^{12} \text{ cm}^{-3}$ and $L_n \sim 4 \text{ cm}$ for both \bar{n}_e cases. Although detailed scans of \bar{n}_e have not yet been carried out

ORNL-DWG 90-2489 FED

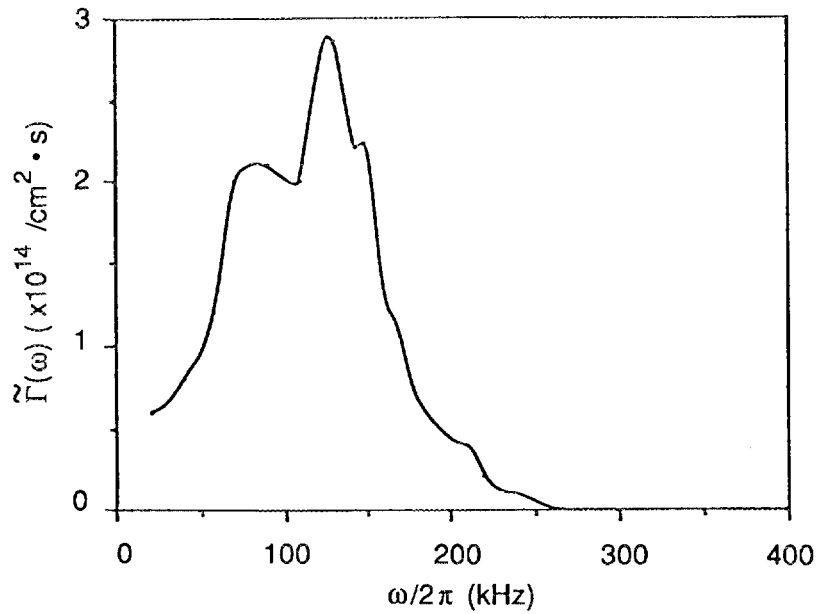


Fig. 7. Typical spectrum of the fluctuation-induced particle flux.

ORNL-DWG 90M-2532 FED

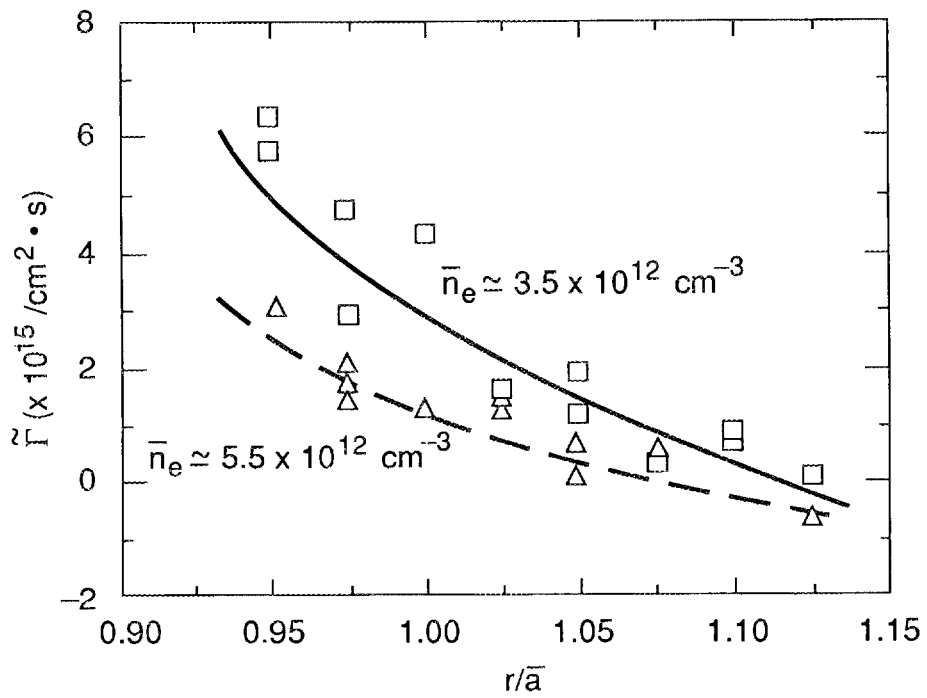


Fig. 8. Spatial profile of the fluctuation-induced particle flux at the edge.

in ATF to determine the scaling of $\tilde{\Gamma}$ with \bar{n}_e , results from the present limited scans indicate that $\tilde{\tau}_p$ increases with \bar{n}_e in these low-density regime studies. This observation is consistent with the TEXT results [15]. In ATF, it is rather difficult to use H_α spectroscopic measurements for estimating the particle fluxes at the edge because of the lack of a full set of spectroscopic monitors to cover the complicated edge geometry and the existence of particle sources from the divertor stripes around the LCFS [16]. Nonetheless, some comparisons can be made. Based on available data from H_α measurements, the estimated particle flux from the particle balance is $\Gamma_{H_\alpha} \sim (1-1.5) \times 10^{15} \text{ cm}^{-2} \cdot \text{s}^{-1}$ for $\bar{n}_e = 5.5 \times 10^{12} \text{ cm}^{-3}$, which is comparable to $\tilde{\Gamma}$. This suggests that the electrostatic edge turbulence may be responsible for particle confinement characteristics in ATF.

A spatial profile of the mean phase velocity of the fluctuations, $v_{ph} = 2\sum_{\omega>0} v_{ph}(\omega)$ with $v_{ph}(\omega) = \sum_k (\omega/k) S(k, \omega) / \sum_k S(k, \omega)$, is given in Fig. 9. As observed on TEXT [2], the propagation of the fluctuations is in the ion diamagnetic direction for $r/\bar{a} > 1$, but it reverses to the electron diamagnetic direction for $r/\bar{a} < 1$. The location of the v_{ph} shear layer nearly coincides with the peak of the plasma potential where the radial electric field $E_r = -d\phi_p/dr$ changes its direction from outward to inward, as shown in Fig. 10 for $\delta_p \sim 2.5$. At this location, the density and electron temperature gradients are nearly

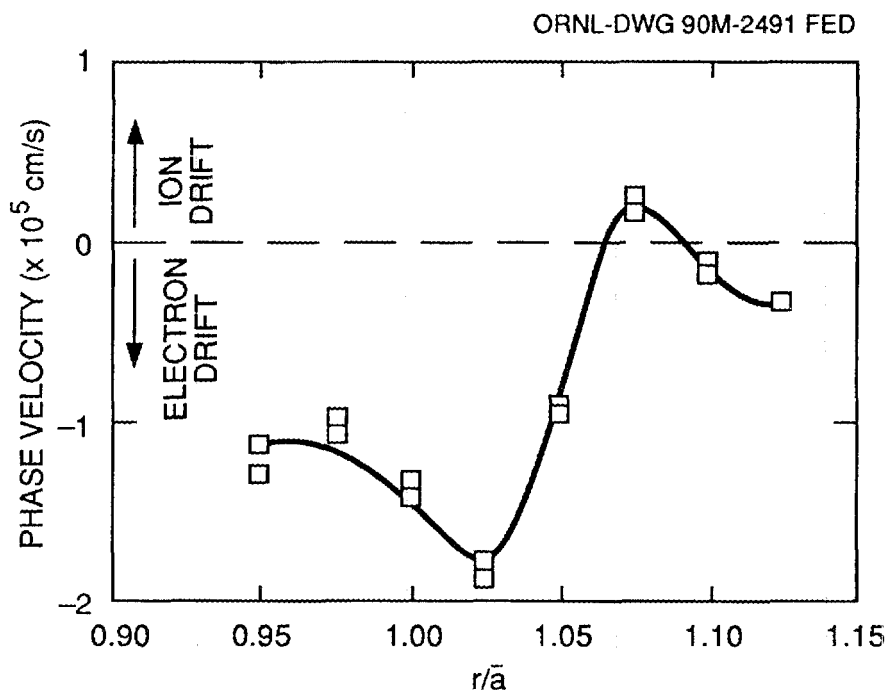


Fig. 9. Spatial profile of the mean phase velocity v_{ph} of the fluctuations. Beyond the shear layer, the wave propagation is in the ion diamagnetic direction.

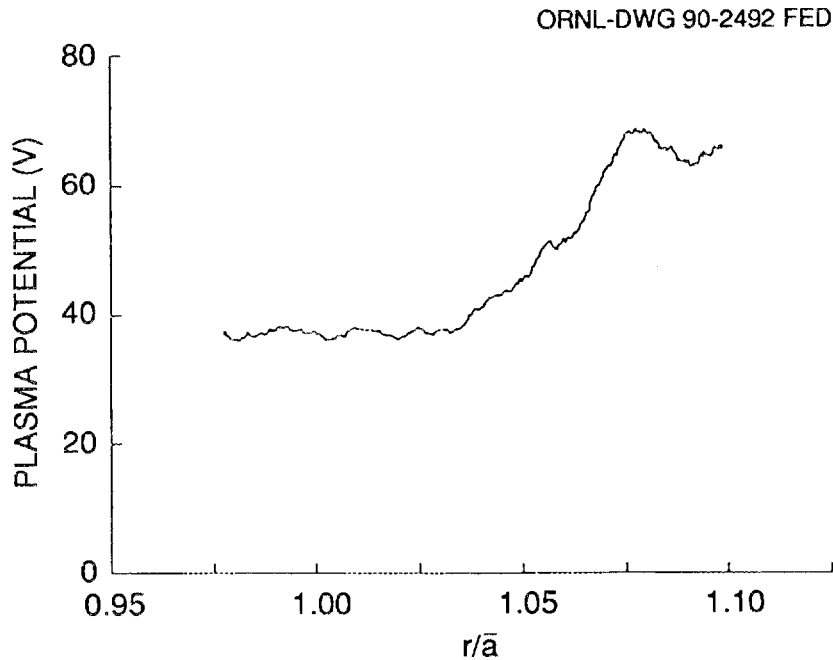


Fig. 10. Spatial profile of the estimated edge plasma potential ϕ_p . The location of the v_{ph} shear layer nearly coincides with the peak of the plasma potential where the radial electric field $E_r = -d\phi_p/dr$ changes its direction from outward to inward.

zero and $v_{ph} \sim v_e \sim 0$, where $v_e = (T_e/eB)(1/L_n + 1/L_T) - E_r/B$ is the electron drift velocity. Also, well inside the LCFS, where $E_r \approx 0$, it is found that $v_{dc} \approx v_{ph} \approx 10^3$ m/s.

Future experiments will include measuring the electron temperature fluctuations using the techniques given in refs. [12,17] to determine the relationship between $\tilde{\phi}_p/T_e$ and \tilde{n}_e/n_e , scaling of the edge fluctuation parameters with \bar{n}_e , and extending the experiments to ECH plasmas with $B = 2$ T and neutral-beam-heated plasmas. The heavy ion beam probe diagnostic [18] should provide additional information on the plasma potential and its fluctuations.

4. CONCLUSION

The initial results indicate substantial similarities in the characteristics of edge turbulence in the ohmically heated TEXT tokamak and the currentless ATF torsatron. The fluctuation-induced particle flux is consistent with the total particle flux estimated from the global particle balance. Thus, electrostatic turbulence may be responsible for

the edge particle transport. Detailed comparison of the ATF and TEXT results can serve as the basis for development of a unified physics interpretation of edge turbulence in toroidal devices.

ACKNOWLEDGMENTS

The authors thank B. A. Carreras, J. N. Leboeuf, P. H. Diamond, and D. R. Thayer for valuable discussions, M. Murakami and the other members of the ATF group and operating staff for help in carrying out the experiments, and J. Sheffield for continual support and encouragement.

REFERENCES

- [1] S. Sudo et al., Nucl. Fusion **30** (1990) 11.
- [2] P. Liewer, Nucl. Fusion **15** (1975) 487.
- [3] Ch. P. Ritz, R. D. Bengtson, S. J. Levinson, and E. J. Powers, Phys. Fluids **27** (1984) 2956; Ch. P. Ritz et al., Nucl. Fusion **27** (1987) 1125.
- [4] J. F. Lyon et al., Fusion Technol. **10** (1986) 179.
- [5] Ch. P. Ritz et al., Phys. Rev. Lett. **62** (1989) 1844.
- [6] Ch. P. Ritz et al., Rev. Sci. Instrum. **61** (1990) 2998; T. L. Rhodes et al., Rev. Sci. Instrum. **61** (1990) 3001.
- [7] T. Uckan et al., Bull. Am. Phys. Soc. **33** (1988) 2069.
- [8] E. J. Powers, Nucl. Fusion **14** (1974) 749.
- [9] J. M. Beall, Y. C. Kim, and E. J. Powers, J. Appl. Phys. **43** (1982) 3993.
- [10] Ch. P. Ritz et al., Rev. Sci. Instrum. **59** (1988) 1739.
- [11] P. C. Stangeby, Plasma sheath, in: Physics of Plasma-Wall Interactions in Controlled Fusion, Eds. D. E. Post and R. Behrisch (Plenum, New York, 1986) p. 41.
- [12] H. Lin, R. D. Bengtson, and Ch. P. Ritz, Univ. of Texas, Report FRCR-334 (1989).
- [13] C. Hidalgo et al., in: Proc. 17th European Conf. Controlled Fusion and Plasma Physics, Amsterdam, 1990 (European Physical Society, 1990), Vol. 14B, p. 1353.
- [14] A. Carlson et al., in: Proc. of the Cadarache Workshop on Electrostatic Turbulence, EUR-CEA-FC-1381 (1989), p. 225.
- [15] W. L. Rowan et al., Nucl. Fusion **27** (1987) 1105.
- [16] P. K. Mioduszewski et al., in: Proc. 16th European Conf. Controlled Fusion and Plasma Physics, Venice, 1989 (European Physical Society, 1989), Vol. 13B, p. 623.
- [17] D. C. Robinson and M. G. Rusbridge, Plasma Phys. **11** (1969) 73.
- [18] A. Carnevali et al., Rev. Sci. Instrum. **59** (1988) 1670.

INTERNAL DISTRIBUTION

1. Director, Fusion Energy Division
2. C. C. Baker
3. M. J. Saltmarsh
4. L. A. Berry
5. B. A. Carreras
6. R. A. Dory
7. J. L. Dunlap
8. H. H. Haselton
9. M. S. Lubell
10. T. E. Shannon
- 11-12. Laboratory Records Department
13. Laboratory Records, ORNL-RC
- 14-15. Central Research Library
16. Document Reference Section
17. Fusion Energy Division Library
- 18-19. Engineering Technology/Fusion Energy Division Publications Office
20. ORNL Patent Office
- 21-30. T. Uckan
31. J. D. Bell
32. L. A. Charlton
33. R. J. Colchin
34. G. R. Dyer
35. G. R. Hanson
36. J. H. Harris
37. D. L. Hillis
38. S. Hiroe
39. L. D. Horton
40. R. C. Isler
41. T. C. Jernigan
42. J. N. Leboeuf
43. J. F. Lyon
44. P. K. Mioduszewski
45. M. Murakami
46. D. A. Rasmussen
47. K. C. Shaing
48. J. B. Wilgen
49. W. R. Wing

EXTERNAL DISTRIBUTION

50. Office of the Assistant Manager for Energy Research and Development, U.S. Department of Energy, Oak Ridge Operations Office, P.O. Box E, Oak Ridge, TN 37831
51. J. D. Callen, Department of Nuclear Engineering, University of Wisconsin, Madison, WI 53706-1687
52. R. W. Conn, Department of Chemical, Nuclear, and Thermal Engineering, University of California, Los Angeles, CA 90024

53. N. A. Davies, Acting Director, Office of Fusion Energy, Office of Energy Research, ER-50 Germantown, U.S. Department of Energy, Washington, DC 20545
54. S. O. Dean, Fusion Power Associates, Inc., 2 Professional Drive, Suite 248, Gaithersburg, MD 20879
55. H. K. Forsen, Bechtel Group, Inc., Research Engineering, P.O. Box 3965, San Francisco, CA 94119
56. R. W. Gould, Department of Applied Physics, California Institute of Technology, Pasadena, CA 91125
57. R. A. Gross, Plasma Research Laboratory, Columbia University, New York, NY 10027
58. D. M. Meade, Princeton Plasma Physics Laboratory, P.O. Box 451, Princeton, NJ 08543
59. M. Roberts, International Programs, Office of Fusion Energy, Office of Energy Research, ER-52 Germantown, U.S. Department of Energy, Washington, DC 20545
60. W. M. Stacey, School of Nuclear Engineering and Health Physics, Georgia Institute of Technology, Atlanta, GA 30332
61. D. Steiner, Nuclear Engineering Department, NES Building, Tibbetts Avenue, Rensselaer Polytechnic Institute, Troy, NY 12181
62. R. Varma, Physical Research Laboratory, Navrangpura, Ahmedabad 380009, India
63. Bibliothek, Max-Planck Institut für Plasmaphysik, Boltzmannstrasse 2, D-8046 Garching, Federal Republic of Germany
64. Bibliothek, Institut für Plasmaphysik, KFA Jülich GmbH, Postfach 1913, D-5170 Jülich, Federal Republic of Germany
65. Bibliothek, KfK Karlsruhe GmbH, Postfach 3640, D-7500 Karlsruhe 1, Federal Republic of Germany
66. Bibliothèque, Centre de Recherches en Physique des Plasmas, Ecole Polytechnique Fédérale de Lausanne, 21 Avenue des Bains, CH-1007 Lausanne, Switzerland
67. H. Renner, Max-Planck Institut für Plasmaphysik, Boltzmannstrasse 2, D-8046 Garching, Federal Republic of Germany
68. Bibliothèque, CEN/Cadarache, F-13108 Saint-Paul-lez-Durance Cedex, France
69. Library, AEA Fusion, Culham Laboratory, Abingdon, Oxfordshire, OX14 3DB, England
70. Library, JET Joint Undertaking, Abingdon, Oxfordshire OX14 3EA, England
71. Library, FOM-Instituut voor Plasmafysica, Rijnhuizen, Edisonbaan 14, 3439 MN Nieuwegein, The Netherlands
72. Library, National Institute for Fusion Science, Chikusa-ku, Nagoya 464-01, Japan
73. Library, International Centre for Theoretical Physics, P.O. Box 586, I-34100 Trieste, Italy
74. Library, Centro Ricerca Energia Frascati, C.P. 65, I-00044 Frascati (Roma), Italy
75. Library, Plasma Physics Laboratory, Kyoto University, Gokasho, Uji, Kyoto 611, Japan
76. Plasma Research Laboratory, Australian National University, P.O. Box 4, Canberra, A.C.T. 2601, Australia
77. Library, Japan Atomic Energy Research Institute, Naka Fusion Research Establishment, 801-1 Mukoyama, Naka-machi, Naka-gun, Ibaraki-ken, Japan
78. G. A. Eliseev, I. V. Kurchatov Institute of Atomic Energy, P.O. Box 3402, 123182 Moscow, U.S.S.R.
79. V. A. Glukhikh, Scientific-Research Institute of Electro-Physical Apparatus, 188631 Leningrad, U.S.S.R.
80. I. Shpigel, Institute of General Physics, U.S.S.R. Academy of Sciences, Ulitsa Vavilova 38, Moscow, U.S.S.R.
81. D. D. Ryutov, Institute of Nuclear Physics, Siberian Branch of the Academy of Sciences of the U.S.S.R., Sovetskaya St. 5, 630090 Novosibirsk, U.S.S.R.
82. O. Pavlichenko, Kharkov Physical-Technical Institute, Academical St. 1, 310108 Kharkov, U.S.S.R.
83. Deputy Director, Southwestern Institute of Physics, P.O. Box 15, Leshan, Sichuan, China (PRC)
84. Director, The Institute of Plasma Physics, P.O. Box 26, Hefei, Anhui, China (PRC)

85. R. A. Blanken, Experimental Plasma Physics Research Branch, Division of Applied Plasma Physics, Office of Energy Research, ER-542, Germantown, U.S. Department of Energy, Washington, DC 20545
86. R. A. E. Bolton, IREQ Hydro-Quebec Research Institute, 1800 Montée-Ste.-Julie, Varennes, P.Q. JOL 2P0, Canada
87. D. H. Crandall, Experimental Plasma Physics Research Branch, Division of Applied Plasma Physics, Office of Energy Research, ER-542, Germantown, U.S. Department of Energy, Washington, DC 20545
88. R. L. Freeman, General Atomics, P.O. Box 85608, San Diego, CA 92138-5608
89. K. W. Gentle, RLM 11.222, Institute for Fusion Studies, University of Texas, Austin, TX 78712
90. R. J. Goldston, Princeton Plasma Physics Laboratory, P.O. Box 451, Princeton, NJ 08543
91. J. C. Hosea, Princeton Plasma Physics Laboratory, P.O. Box 451, Princeton, NJ 08543
92. A. J. Wootton, Fusion Research Center, The University of Texas, Austin, TX 78712.
93. R. H. McKnight, Experimental Plasma Physics Research Branch, Division of Applied Plasma Physics, Office of Energy Research, ER-542, Germantown, U.S. Department of Energy, Washington, DC 20545
94. E. Oktay, Division of Confinement Systems, Office of Energy Research, ER-55, Germantown, U.S. Department of Energy, Washington, DC 20545
95. R. R. Parker, Plasma Fusion Center, NW 16-288, Massachusetts Institute of Technology, Cambridge, MA 02139
96. W. L. Sadowski, Fusion Theory and Computer Services Branch, Division of Applied Plasma Physics, Office of Energy Research, ER-541, Germantown, U.S. Department of Energy, Washington, DC 20545
97. J. W. Willis, Division of Confinement Systems, Office of Energy Research, ER-55, Germantown, U.S. Department of Energy, Washington, DC 205
98. A. Perez Navarro, Division de Fusion, CIEMAT, Avenida Complutense 22, E-28040 Madrid, Spain
99. Laboratory for Plasma and Fusion Studies, Department of Nuclear Engineering, Seoul National University, Shinrim-dong, Gwanak-ku, Seoul 151, Korea
100. J. L. Johnson, Plasma Physics Laboratory, Princeton University, P.O. Box 451, Princeton, NJ 08543
101. L. M. Kovrizhnykh, Institute of General Physics, U.S.S.R. Academy of Sciences, Ulitsa Vavilova 38, 117924 Moscow, U.S.S.R.
102. O. Motojima, National Institute for Fusion Science, Chikusa-ku, Nagoya 464-01, Japan
103. S. Okamura, Institute of Plasma Physics, Nagoya University, Chikusa-ku, Nagoya 464, Japan
104. V. D. Shafranov, I. V. Kurchatov Institute of Atomic Energy, P.O. Box 3402, 123182 Moscow, U.S.S.R.
105. J. L. Shohet, Torsatron/Stellarator Laboratory, University of Wisconsin, Madison, WI 53706
106. H. Wobig, Max-Planck Institut für Plasmaphysik, D-8046 Garching, Federal Republic of Germany
107. F. S. B. Anderson, University of Wisconsin, Madison, WI 53706
108. R. F. Gandy, Physics Department, Auburn University, Auburn, AL 36849-3511
109. C. Hidalgo-Vera, Division de Fusion, CIEMAT, Avenida Complutense 22, E-28040 Madrid, Spain
110. H. Kaneko, Plasma Physics Laboratory, Kyoto University, Gokasho, Uji, Japan
111. G. H. Neilson, Princeton Plasma Physics Laboratory, P.O. Box 451, Princeton, NJ 08543
112. Ch. P. Ritz, Fusion Research Center, University of Texas, Austin, TX 78712
113. S. Sudo, Plasma Physics Laboratory, Kyoto University, Gokasho, Uji, Kyoto 611, Japan
114. C. E. Thomas, Georgia Institute of Technology, Atlanta, GA 30332
115. H. Yamada, National Institute for Fusion Science, Chikusa-ku, Nagoya 464-01, Japan
116. J. Tachon, CEN/Cadarache, Departement de Recherches sur la Fusion Contrôlée, F-13108 Saint-Paul-lez-Durance, France
117. F. W. Perkins, Princeton Plasma Physics Laboratory, P.O. Box 451, Princeton, NJ 08543

118. T. Obiki, Plasma Physics Laboratory, Kyoto University, Gokasho, Uji, Kyoto, Japan
119. A. Iiyoshi, National Institute for Fusion Studies, Chikusa-ku, Nagoya 464-01, Japan
- 120--172. Given distribution as shown in OSTI-4500, Magnetic Fusion Energy (Category Distribution UC-426, Experimental Plasma Physics) (53 copies)